CHARACTERIZATION OF THE GROWTH AND EMISSION PROPERTIES OF HYBRID CARBON FILMS CONTAINING CARBON NANOTUBES

V. Ayres, B. Wright, J. Asmussen, S. Song, S. Khatami, D. Reinhard, and D. Tomanek
Michigan State University, East Lansing, MI, 48824

D. Roach
DuPont Experimental Station, Wilmington, DE, 19880

Abstract

We report our recent progress in the synthesis and characterization of hybrid carbon films produced by microwave plasma-enhanced chemical vapor deposition. Hybrid carbon films contain multiple allotropes of carbon in the same film by design, i.e. diamond plus carbon nanotubes. Such films may be of particular interest for applications in field emission displays. A current research issue in field-induced emission mechanisms is the possible role which local field enhancement from sharp geometrical structures plays in electron emission versus the role of the electronic states at an sp^2 / sp^3 interface. In these experiments, we investigate this issue in the context of the observed growth morphologies.

INTRODUCTION

We report on our recent progress in the synthesis and characterization of hybrid carbon films produced by microwave plasma-enhanced chemical vapor deposition. Hybrid carbon films contain multiple allotropes of carbon in the same films by design, i.e., diamond plus carbon nanotubes. Carbon films are of particular interest in for flat panel display applications. Diamond (Ref. (1)), tetrahedral amorphous carbon (Refs. (2)) and carbon nanotubes (Ref. (3) and Ref. (4)) all exhibit low threshold electron emission behavior. However, the mechanism, or combination of mechanisms, by which the emission takes place are not well understood. Such understanding is key to the control of problems which currently impede the success of carbon films in emission applications, such as non-uniform emission site density across a single film, or variable emission performance from "identically" grown films.

A current research issue in field-induced electron emission mechanisms in carbon films is the possible role which local field enhancement from sharp geometrical structures plays versus the possible role of electronic states at an sp^2/sp^3 interface which are favorable for emission. Investigations of carbon nanotubes indicate that geometric field enhancement should result in excellent emission properties (Ref. (5) and Ref. (6)). However, experimental investigations of single (Ref. (3)) and multi-walled (Ref. (4)) carbon nanotube films show that problems remain, with nonuniform emission site densities and a turn-on threshold which, while low, is about an order of magnitude higher than would be desirable for commercial applications.

Other carbon films composed of more complicated carbon nano-structures which may contain carbon nanotubes, have also shown excellent emission properties (Ref. (7) and Ref. (8)). Such films are currently under investigation to determine whether materials with mixed sp^2/sp^3 bonded phases emit electrons more easily and have a higher emission site density that pure phase materials. Also, a correlation has also been noted between the ratio of I_D, the disorder peak and I_G, the graphitic peak, as measured by Raman spectroscopy, and better emission properties: a low I_D/I_G seems to correlate with a low electron emission threshold (Ref. (7)).

Our group is investigating these issues. Using microwave plasma-enhanced chemical vapor deposition under carefully controlled conditions, we deposit carbon films, which range form pure phase carbon allotropes through hybrid carbon forms. The morphology and hybridization(s) of the films are characterized, and correlated with their electron emission performance. In this paper, we report on the growth, characterization and first emission results from two series of hybrid carbon films, which can be linked directly to the pure phase diamond depositions.

EXPERIMENTAL

Depositions

A 2.45 GHz microwave plasma cavity reactor with a 12.5 centimeter maximum discharge was used to deposit the hybrid carbon films on 7.62 centimeter p-type (100) silicon wafers. The Michigan State University microwave plasma reactor system is combined with a computer controlled ultrahigh vacuum and gas handling system which allowed careful control of the gas input variables. However, for the first set of experiments, the leak rates were not systematically investigated and must be regarded as unknown. For the second set of experiments, the leak rates were systematically investigated and typical leak rates were approximately 0.25 mTorr/hour.

Input gases of research and ultrahigh purity, hydrogen-99.9995%, and methane-99.99% were used in all experiments. The first set of experiments did not involve the explicit introduction of nitrogen, but unknown quantities of nitrogen may have been present due to leakage. For the second set of experiments, parts per million (ppm) of nitrogen were deliberately introduced via a pre-mixed gas of 2% N_2 in H_2, which had a purity of 99.9995%. Gas phase nitrogen concentrations were monitored by optical emission spectroscopy (OES), by using the CN emission band. Based on our calibration experiments, we give an estimate of 5 ppm nitrogen concentration as our "0" ppm nitrogen concentration for the second set of experiments.

In these experiments, the reactor was operated in thermally floating configuration with the substrate temperature mainly dependent on the operating pressure (Ref (9)). Our calibration experiments showed that at an operating pressure of 50.4 Torr, the substrate temperature was approximately 900°C. The actual temperatures were also measured by a single color optical pyrometer.

Analyses

A. Surface Morphology

Atomic force microscopy (AFM) was used to investigate surface features below five microns, while Scanning Electron Microscopy (SEM) was for larger areas. The AFM imaging was performed using a Digital Instruments™ Nanoscope IIIa operated in TappingMode® in ambient air. Etched silicon tips with a nominal tip radius of 5-10 nm were used for all images. All images shown were acquired using the "E" scanner (13 μm x 13 μm).

B. Raman Spectroscopy

The Raman spectroscope used in these experiments consisted of a 0.75 m double monochromator coupled with an optical microscope, operated in backscattering configuration. An argon ion laser was used as the excitation source. The excitation wavelength was 514.5 nm, the spot size was approximately 10 μm in diameter, and the laser power at the sample surface was approximately 30 mW.

The Raman spectra were deconvolved into individual spectral peak components using the Method of Residuals with Lorentz lineshape amplitudes. For all spectra with one exception (0.94), the coefficient of determination

$$r^2 = 1 - \frac{\text{Sum of squares due to error}}{\text{Sum of squares about the mean}} \quad [1]$$

was 0.95 or greater, where 1.0 is a perfect to the data.

RESULTS

In the first set of experiments, an unusual carbon morphology was observed under deposition conditions, specifically pressure and methane/hydrogen ratio conditions, which differed only slightly form those which produced polycrystalline diamond films: 50.4 Torr versus 38.4 Torr and ~ 4% CH_4/H_2 versus 2% CH_4/H_2. The appearance of these films was dark and matte instead of light and reflective. The morphology of the dark material was not consistent with the usual graphitic or "ballas-like" diamond often observed in diamond depositions which correlates with a large sp^2 component. The appearance of the new morphology was "grass-like" with some sub-structure, which was difficult to resolve by SEM. Raman spectroscopy confirmed that the signature diamond triple phonon peak at 1332.5 cm^{-1} was not present in these films. Instead, two broad peaks were observed at about 1350 cm^{-1} and near 1600 cm^{-1}. These peaks were identified as the "I_D" and I_G" peaks but were not further deconvolved. The ratio of I_D/I_G for these samples is given in Table I. Electron emission measurements from these samples, still underway, indicate a rough correlation between the low I_D/I_G films and better electron emission.

The first series of growths corresponded to a study of the film properties as a function of increasing CH_4/H_2. However, the plasma was hand-tuned to produce the appearance of a uniform plasma ball over the substrate. In so doing, the pressure/temperature and the input power parameters were also changed. Also, these first depositions contained unknown amounts of atmospheric nitrogen. A second set of experiments to explicitly study the new morphology was undertaken. In the second series of experiments, the pressure was held constant at 50.4 Torr, the input power was held constant at 2.5 kW, and the CH_4/H_2 ratio was held constant at 2%. The reactor was carefully sealed and the leak rate, established at ~ 0.25 mTorr/hour, was systematically monitored by OES. The only variable introduced was parts per million of nitrogen as this has been shown by our group and others to have a strong effect on diamond morphology and texture (Refs. (10)).

Our results were as follows. A dark matte spot was present in depositions with 0, 25, 50, 200 and 400 ppm nitrogen. This time it was noted that a lighter reflective material surrounded the dark matte material. For low nitrogen concentrations, 0, 25 and 50 ppm, this was a central dark spot surrounded symmetrically by a ring of lighter, reflective material as shown in Figure 1a. For higher ppm nitrogen, the deposition broke up as shown in Figure 1b. AFM investigation of the bright reflective material showed a ballas-like morphology for the low ppm depositions which changed into (100) faceted diamond for the higher ppm nitrogen concentrations (diamond confirmed by Raman spectroscopy). An image of the (100) faceted diamond is shown in Figure 2a.

SEM and AFM investigation of the dark matte spots showed the same type of new morphology observed in the first series of depositions. The macroscopic appearance of the dark material is shown in Figure 2b. Similar morphologies have been reported in Refs. (7) and (8). In Ref. (7) the material is described as oriented carbon nanostructures and was grown under conditions appropriate for nanotube growth, included a metallic catalyst. In Ref. (8) the material is described as nanocorraline diamond and was grown under conditions appropriate for diamond growth

A close-up of an individual structure shown in Figure 2c indicates a sub-structure with about 20 nm repeats. Although no conclusions are drawn, a morphology of a similar "wrapped" appearance is sometime observed in dense dispersion of single walled nanotubes in addition to the more common ropes. Examples of such morphologies, resulting from dense dispersions of Tubes@Rice single walled nanotubes are shown in Figure 3.

AFM and SEM investigation of the dark material did not indicate any systematic change in the nanostructured morphology as a function of increasing ppm nitrogen, unlike the strong effect of nitrogen on the lighter surrounding material. However, at 400 ppm nitrogen, clusters of nanostructured material were observed, as shown in Fig 4a. For comparison, the (100) faceted diamond surrounding material is shown in Figure 4b. Both carbon forms are from the same plasma deposition.

Raman spectroscopy and analysis was performed on both the dark matte and light reflective areas of the second series of depositions. Representative results are shown in Figure 5. All dark matte areas showed a strong "D" peak at about 1350 cm^{-1}, with lesser

peaks nearby as shown in Figure 5a. However, careful study and deconvolution of the "G" peak indicated a strong peak at about 1590 cm^{-1}, with three lesser peaks shown in Figure 5a. This is not the usual "G" peak discussed in diamond growth references. In diamond depositions the "G" peak occurs near1580 cm^{-1} and is usually identified with the stretching and shear modes of *planar* graphite (Refs. (11) and Ref. (12)). Raman spectroscopy of carbon nanotubes shows a strong peak at about 1590 cm^{-1} which is identified with an E_{2g} stretching mode, and it also shows a group of nearby lesser peaks (Ref. (13)).

Raman analysis of the bright reflective areas for the low ppm nitrogen depositions with 0, 25 and 50 ppm nitrogen showed a very broad multi-componnet peak, as shown in Figure 5b. The location of the broad peak's center varied between about 1330 cm^{-1} and 1450 cm^{-1}. A strong peak at 1590 cm^{-1} was not observed for any of these samples. Raman spectroscopy of amorphous carbon usually exhibits one or two very broad peaks at about 1370 cm^{-1} and 1530 cm^{-1}, but the peak positions, widths and intensities vary greatly as a function of different sp^2/sp^3, hydrogen, etc. content in the films.

Raman analysis of the bright reflective material for the high ppm depositions with 200 and 400 ppm nitrogen showed a clear strong diamond component peak near 1332.5 cm^{-1}, as shown in Figure 5c. This result correlates with the observed (100) well-faceted morphology. A strong component at 1590 cm^{-1} was not observed in any of these samples.

SUMMARY AND CONCLUSIONS

In this work, we report on growth and emission results from a nanostructured carbon material. Two types of carbon materials, one dark, matte and nanostructured, and the other light, reflective, and, for higher ppm nitrogen, crystalline, are deposited from same plasma. This suggests that two very different plasma chemistries are present in different regions of the same plasma ball. AFM and Raman results suggest that for the low ppm nitrogen depositions, the reflective material could be the ballas-like graphitic material observed in diamond depositions. It is known that this type of material can be converted into well-faceted (100) diamond material with the addition of ppm of nitrogen (Refs. (10)). Such a phenomenon may have occurred in these depositions, without, however, similarly converting the dark nanostructured material into diamond. The morphology and Raman analysis of the dark matte material suggest that it may contain a carbon nanotube component. However, this needs further investigation. No metallic catalyst was present in these depositions. Further Raman investigations are underway, using filtered green 514.5 nm and also red 632.8 nm laser excitations to determine whether radial breathing modes are observed in the dark matte samples.

First electron emission results seemed to show a correlation between better emission and low I_D/I_G, similar to that reported by other authors. However, we find that the I_D/I_G ratio is differently defined in different references. Our future work will explore these differences more closely.

TABLE I. Deposition conditions which produced the first series of nanostructured films.

Sample	Pressure (Torr)	Input Power (kW)	CH_4/H_2 (%)	Temperature (°C)	I_D/I_G
SK-35	49	1.4	2.75	900	1.8
SK-37	52	1.6	2.75	950	2.1
SK-42	47	1.6	3.75	900	2.7
SK-43	52	1.8	3.75	950	2.8
SK-44	58	2.0	3.75	1000	1.5
SK-47	57	2.1	4.75	1000	1.3

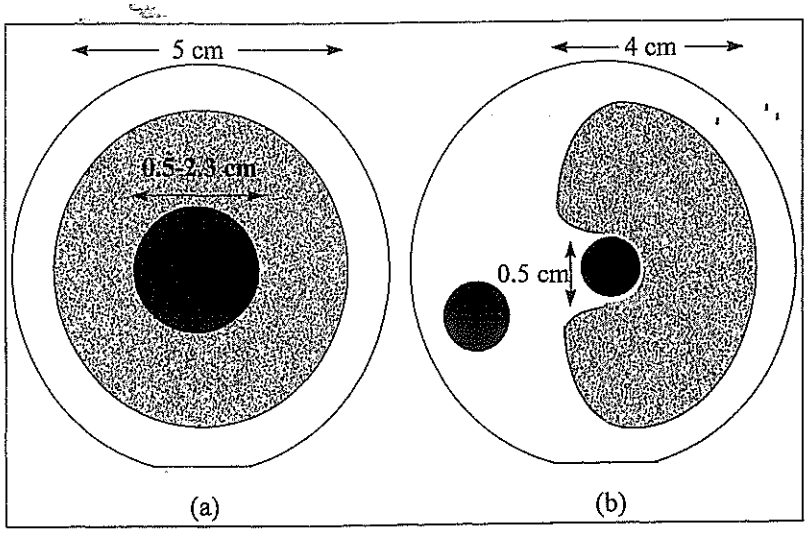

Figure 1. Depositions as a function of ppm N_2 (a) 0, 25 and 50 ppm N_2, and (b) 200 and 400 ppm N_2.

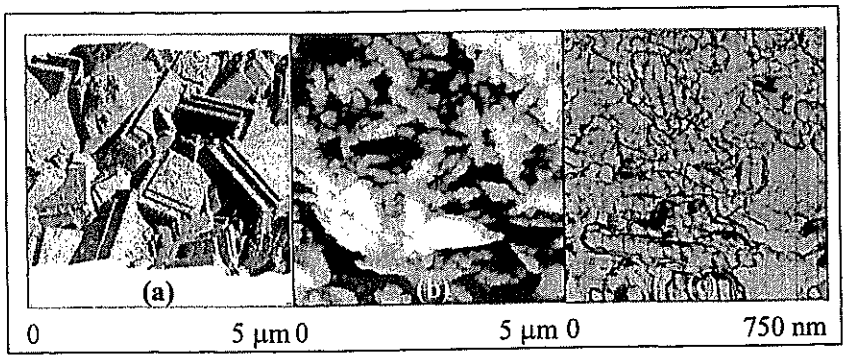

Figure 2. TappingMode™ AFM images of representative surface morphologies from the (a) crystalline and (b) graphitic areas of the depositions. (c) A close-up phase image of the graphitic morphology, showing details of the structure.

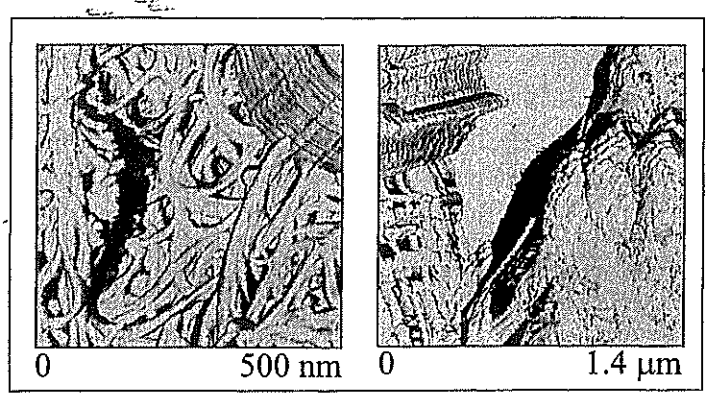

Figure 3. TappingMode™ AFM phase images of dense dispersions of Tubes@Rice carbon nanotubes showing striated arrangements as well as bundled nanotube ropes.

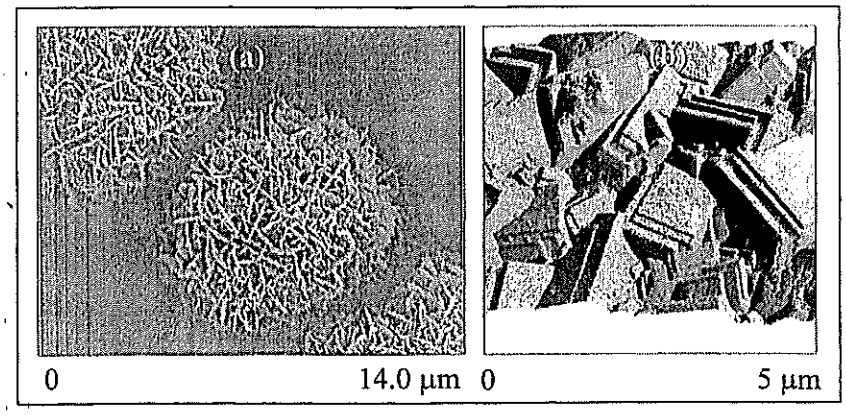

Figure 4. Observed morphologies of central graphitic "dark spot" and bright, relective surrounding deposition for 2% methane-hydrogen, 50.4 torr and 400 ppm nitrogen. (a) SEM image of graphitic morphology shows clusters of nanoscale material. (b) Tapping Mode™ AFM image of surrounding deposition shows a well-faceted crystalline material. Based on appearance and Raman measurement, the material is (100)-faceted diamond.

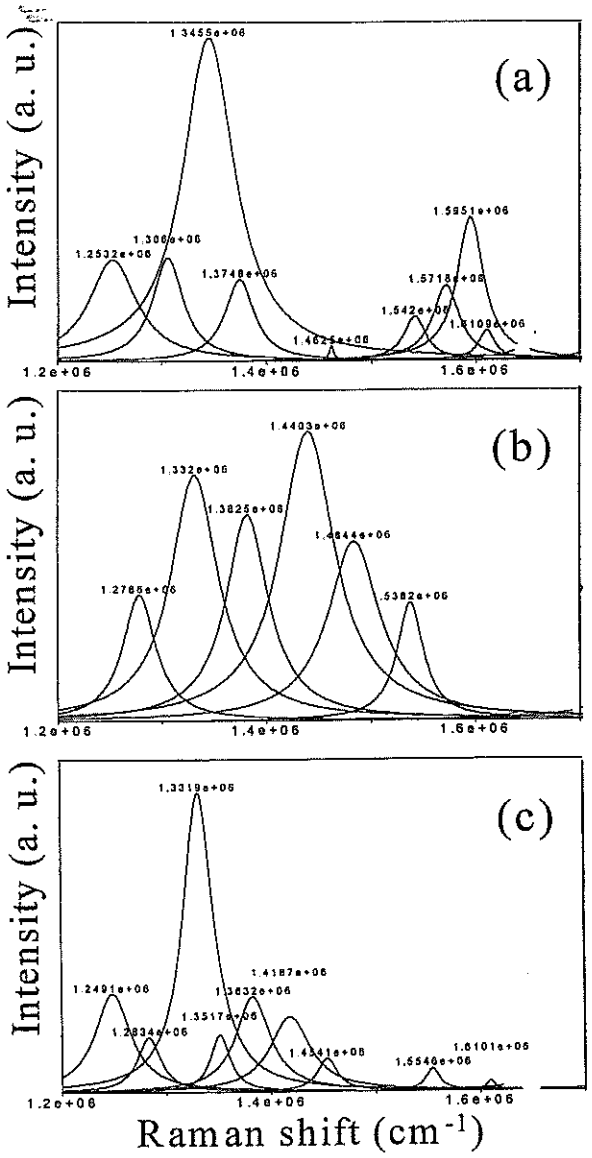

Figure 5. Typical Raman spectra for (a) the central graphitic "dark spot", (b) the bright, relective surrounding deposition for low ppm nitrogen, 0 through 50 ppm, and (c) the bright relective surrounding deposition for higher ppm nitrogen, 200 and 400 ppm.

REFERENCES

1. K. Okano, S. Koizumi, S. Ravi, P. Silva and G. A. J. Amaratunga, Nature, **381**, p. 140 (1996).

2. A. Hart, B. S. Satanaryana, W. I. Milne and J. Robertson, Carbon **37**, p. 759 (1999); C. W. Chen and J. Robertson, J. Vac Sci Technol B **17**, p. 659 (1999); A C Ferrari, B S Satyanayana, J Robertson, W I Milne, E Barborini, P Piseri, P Milani, Euorphys Lett. **46**, p. 245 (1999).

3. W. B. Choi, Y. H. Lee, D. S. Chung, N. S. Lee and J. M. Kim, in *Proceedings of the 1999 International Workshop on Science and Application of Nanotubes,* D. Tomanek and R. Enbody, Editors. p. 361, Fundamental Materials Research Series, Kluwer Academic (2000).

4. Y. Saito and S. Uemura, Carbon **38**, p. 169 (2000).

5. O. Groening, O. M. Kuttel, Ch. Emmenegger, P. Groening and L. Schlapach, J. Vac Sci Technol B **17**, p. 400 (1999).

6. A. G. Rinzler, J. H. P. Nicolaev, L. Lou, S. G. Kim, D. Tomanek, P. Norlander, D. T. Colbert and R. Smalley, Science **269**, p. 1550 (1995).

7. A. M. Bonnot, M. N. Semeria, J. F. Boronat, T. Fournier and L. Pontonnier, in press, Diamond and Related Materials (2000).

8. B. F. Coll, J. E. Jaskie, J. L. Markham, E. P. Menu, A. A. Talin and P. von Allmen, Mat. Research Soc. Symp. Proc. Vol. **498**, p. 185 (1998).

9. S. Khatami, Thesis: Controlled Synthesis of Diamond Films Using a Microwave Plasma Discharge Reactor, Michigan State University (1997).

10. V. M. Ayres, T. R. Bieler, M. G. Kanatzidis, S. Hagopian, B. L. Wright and J. Asmussen, in press, Diamond and Relat. Mater. (2000); J. Asmussen, J. Mossbrucker, S. Khatami, W. S. Huang. B. Wright and V. M. Ayres, Diamond and Relat. Mater., Vol. **8**, p. 220 (1999).

11. M. Yoshikawa, G. Katagiri, H. Ishida, A. Ishitani, M. Ono, and K. Matsumura, App. Phys. Lett. **55**, p. 2608 (1989).

12. D. S. Knight and W. B. White, J. Mater. Res., Vol. **4**, p. 385 (1989).

13. R. Saito, G. Dresselhaus, and M. Dresselhaus, *Physical Properties of Carbon Nanotubes*, Chapter 10, Imperial College Press, distributed by World Scientific Publishing Co. Pte. Ltd., Singapore (1998).